Event-by-event $\langle p_t \rangle$ fluctuations in Au-Au collisions at $\sqrt{s_{NN}} = 130$ GeV

J. Adams,[3] C. Adler,[12] M.M. Aggarwal,[25] Z. Ahammed,[28] J. Amonett,[17] B.D. Anderson,[17] M. Anderson,[5] D. Arkhipkin,[11] G.S. Averichev,[10] S.K. Badyal,[16] J. Balewski,[13] O. Barannikova,[28,10] L.S. Barnby,[17] J. Baudot,[15] S. Bekele,[24] V.V. Belaga,[10] R. Bellwied,[41] J. Berger,[12] B.I. Bezverkhny,[43] S. Bhardwaj,[29] P. Bhaskar,[38] A.K. Bhati,[25] H. Bichsel,[40] A. Billmeier,[41] L.C. Bland,[2] C.O. Blyth,[3] B.E. Bonner,[30] M. Botje,[23] A. Boucham,[34] A. Brandin,[21] A. Bravar,[2] R.V. Cadman,[1] X.Z. Cai,[33] H. Caines,[43] M. Calderón de la Barca Sánchez,[2] J. Carroll,[18] J. Castillo,[18] M. Castro,[41] D. Cebra,[5] P. Chaloupka,[9] S. Chattopadhyay,[38] H.F. Chen,[32] Y. Chen,[6] S.P. Chernenko,[10] M. Cherney,[8] A. Chikanian,[43] B. Choi,[36] W. Christie,[2] J.P. Coffin,[15] T.M. Cormier,[41] J.G. Cramer,[40] H.J. Crawford,[4] D. Das,[38] S. Das,[38] A.A. Derevschikov,[27] L. Didenko,[2] T. Dietel,[12] X. Dong,[32,18] J.E. Draper,[5] F. Du,[43] A.K. Dubey,[14] V.B. Dunin,[10] J.C. Dunlop,[2] M.R. Dutta Majumdar,[38] V. Eckardt,[19] L.G. Efimov,[10] V. Emelianov,[21] J. Engelage,[4] G. Eppley,[30] B. Erazmus,[34] M. Estienne,[34] P. Fachini,[2] V. Faine,[2] J. Faivre,[15] R. Fatemi,[13] K. Filimonov,[18] P. Filip,[9] E. Finch,[43] Y. Fisyak,[2] D. Flierl,[12] K.J. Foley,[2] J. Fu,[42] C.A. Gagliardi,[35] M.S. Ganti,[38] T.D. Gutierrez,[5] N. Gagunashvili,[10] J. Gans,[43] L. Gaudichet,[34] M. Germain,[15] F. Geurts,[30] V. Ghazikhanian,[6] P. Ghosh,[38] J.E. Gonzalez,[6] O. Grachov,[41] V. Grigoriev,[21] S. Gronstal,[8] D. Grosnick,[37] M. Guedon,[15] S.M. Guertin,[6] A. Gupta,[16] E. Gushin,[21] T.J. Hallman,[2] D. Hardtke,[18] J.W. Harris,[43] M. Heinz,[43] T.W. Henry,[35] S. Heppelmann,[26] T. Herston,[28] B. Hippolyte,[43] A. Hirsch,[28] E. Hjort,[18] G.W. Hoffmann,[36] M. Horsley,[43] H.Z. Huang,[6] S.L. Huang,[32] T.J. Humanic,[24] G. Igo,[6] A. Ishihara,[36] P. Jacobs,[18] W.W. Jacobs,[13] M. Janik,[39] I. Johnson,[18] P.G. Jones,[3] E.G. Judd,[4] S. Kabana,[43] M. Kaneta,[18] M. Kaplan,[7] D. Keane,[17] J. Kiryluk,[6] A. Kisiel,[39] J. Klay,[18] S.R. Klein,[18] A. Klyachko,[13] D.D. Koetke,[37] T. Kollegger,[12] A.S. Konstantinov,[27] M. Kopytine,[17] L. Kotchenda,[21] A.D. Kovalenko,[10] M. Kramer,[22] P. Kravtsov,[21] K. Krueger,[1] C. Kuhn,[15] A.I. Kulikov,[10] A. Kumar,[25] G.J. Kunde,[43] C.L. Kunz,[7] R.Kh. Kutuev,[11] A.A. Kuznetsov,[10] M.A.C. Lamont,[3] J.M. Landgraf,[2] S. Lange,[12] C.P. Lansdell,[36] B. Lasiuk,[43] F. Laue,[2] J. Lauret,[2] A. Lebedev,[2] R. Lednický,[10] V.M. Leontiev,[27] M.J. LeVine,[2] C. Li,[32] Q. Li,[41] S.J. Lindenbaum,[22] M.A. Lisa,[24] F. Liu,[42] L. Liu,[42] Z. Liu,[42] Q.J. Liu,[40] T. Ljubicic,[2] W.J. Llope,[30] H. Long,[6] R.S. Longacre,[2] M. Lopez-Noriega,[24] W.A. Love,[2] T. Ludlam,[2] D. Lynn,[2] J. Ma,[6] Y.G. Ma,[33] D. Magestro,[24] S. Mahajan,[16] L.K. Mangotra,[16] D.P. Mahapatra,[14] R. Majka,[43] R. Manweiler,[37] S. Margetis,[17] C. Markert,[43] L. Martin,[34] J. Marx,[18] H.S. Matis,[18] Yu.A. Matulenko,[27] T.S. McShane,[8] F. Meissner,[18] Yu. Melnick,[27] A. Meschanin,[27] M. Messer,[2] M.L. Miller,[43] Z. Milosevich,[7] N.G. Minaev,[27] C. Mironov,[17] D. Mishra,[14] J. Mitchell,[30] B. Mohanty,[38] L. Molnar,[28] C.F. Moore,[36] M.J. Mora-Corral,[19] V. Morozov,[18] M.M. de Moura,[41] M.G. Munhoz,[31] B.K. Nandi,[38] S.K. Nayak,[16] T.K. Nayak,[38] J.M. Nelson,[3] P. Nevski,[2] V.A. Nikitin,[11] L.V. Nogach,[27] B. Norman,[17] S.B. Nurushev,[27] G. Odyniec,[18] A. Ogawa,[2] V. Okorokov,[21] M. Oldenburg,[18] D. Olson,[18] G. Paic,[24] S.U. Pandey,[41] S.K. Pal,[38] Y. Panebratsev,[10] S.Y. Panitkin,[2] A.I. Pavlinov,[41] T. Pawlak,[39] V. Perevoztchikov,[2] W. Peryt,[39] V.A. Petrov,[11] S.C. Phatak,[14] R. Picha,[5] M. Planinic,[44] J. Pluta,[39] N. Porile,[28] J. Porter,[2] A.M. Poskanzer,[18] M. Potekhin,[2] E. Potrebenikova,[10] B.V.K.S. Potukuchi,[16] D. Prindle,[40] C. Pruneau,[41] J. Putschke,[19] G. Rai,[18] G. Rakness,[13] R. Raniwala,[29] S. Raniwala,[29] O. Ravel,[34] R.L. Ray,[36] S.V. Razin,[10,13] D. Reichhold,[28] J.G. Reid,[40] G. Renault,[34] F. Retiere,[18] A. Ridiger,[21] H.G. Ritter,[18] J.B. Roberts,[30] O.V. Rogachevski,[10] J.L. Romero,[5] A. Rose,[41] C. Roy,[34] L.J. Ruan,[32,2] R. Sahoo,[14] I. Sakrejda,[18] S. Salur,[43] J. Sandweiss,[43] I. Savin,[11] J. Schambach,[36] R.P. Scharenberg,[28] N. Schmitz,[19] L.S. Schroeder,[18] K. Schweda,[18] J. Seger,[8] D. Seliverstov,[21] P. Seyboth,[19] E. Shahaliev,[10] M. Shao,[32] M. Sharma,[25] K.E. Shestermanov,[27] S.S. Shimanskii,[10] R.N. Singaraju,[38] F. Simon,[19] G. Skoro,[10] N. Smirnov,[43] R. Snellings,[23] G. Sood,[25] P. Sorensen,[6] J. Sowinski,[13] H.M. Spinka,[1] B. Srivastava,[28] S. Stanislaus,[37] R. Stock,[12] A. Stolpovsky,[41] M. Strikhanov,[21] B. Stringfellow,[28] C. Struck,[12] A.A.P. Suaide,[41] E. Sugarbaker,[24] C. Suire,[2] M. Šumbera,[9] B. Surrow,[2] T.J.M. Symons,[18] A. Szanto de Toledo,[31] P. Szarwas,[39] A. Tai,[6] J. Takahashi,[31] A.H. Tang,[2,23] D. Thein,[6] J.H. Thomas,[18] V. Tikhomirov,[21] M. Tokarev,[10] M.B. Tonjes,[20] T.A. Trainor,[40] S. Trentalange,[6] R.E. Tribble,[35] M.D. Trivedi,[38] V. Trofimov,[21] O. Tsai,[6] T. Ullrich,[2] D.G. Underwood,[1] G. Van Buren,[2] A.M. VanderMolen,[20] A.N. Vasiliev,[27] M. Vasiliev,[35] S.E. Vigdor,[13] Y.P. Viyogi,[38] W. Waggoner,[8] F. Wang,[28] G. Wang,[17] X.L. Wang,[32] Z.M. Wang,[32] H. Ward,[36] J.W. Watson,[17] R. Wells,[24] G.D. Westfall,[20] C. Whitten Jr.,[6] H. Wieman,[18] R. Willson,[24] S.W. Wissink,[13] R. Witt,[43] J. Wood,[6] J. Wu,[32] N. Xu,[18] Z. Xu,[2] Z.Z. Xu,[32] A.E. Yakutin,[27] E. Yamamoto,[18] J. Yang,[6] P. Yepes,[30] V.I. Yurevich,[10] Y.V. Zanevski,[10] I. Zborovský,[9] H. Zhang,[43,2] H.Y. Zhang,[17] W.M. Zhang,[17] Z.P. Zhang,[32] P.A. Żołnierczuk,[13] R. Zoulkarneev,[11] J. Zoulkarneeva,[11] and A.N. Zubarev[10]

(STAR Collaboration)

[1] *Argonne National Laboratory, Argonne, Illinois 60439*

[2]Brookhaven National Laboratory, Upton, New York 11973
[3]University of Birmingham, Birmingham, United Kingdom
[4]University of California, Berkeley, California 94720
[5]University of California, Davis, California 95616
[6]University of California, Los Angeles, California 90095
[7]Carnegie Mellon University, Pittsburgh, Pennsylvania 15213
[8]Creighton University, Omaha, Nebraska 68178
[9]Nuclear Physics Institute AS CR, Řež/Prague, Czech Republic
[10]Laboratory for High Energy (JINR), Dubna, Russia
[11]Particle Physics Laboratory (JINR), Dubna, Russia
[12]University of Frankfurt, Frankfurt, Germany
[13]Indiana University, Bloomington, Indiana 47408
[14]Insitute of Physics, Bhubaneswar 751005, India
[15]Institut de Recherches Subatomiques, Strasbourg, France
[16]University of Jammu, Jammu 180001, India
[17]Kent State University, Kent, Ohio 44242
[18]Lawrence Berkeley National Laboratory, Berkeley, California 94720
[19]Max-Planck-Institut für Physik, Munich, Germany
[20]Michigan State University, East Lansing, Michigan 48824
[21]Moscow Engineering Physics Institute, Moscow Russia
[22]City College of New York, New York City, New York 10031
[23]NIKHEF, Amsterdam, The Netherlands
[24]Ohio State University, Columbus, Ohio 43210
[25]Panjab University, Chandigarh 160014, India
[26]Pennsylvania State University, University Park, Pennsylvania 16802
[27]Institute of High Energy Physics, Protvino, Russia
[28]Purdue University, West Lafayette, Indiana 47907
[29]University of Rajasthan, Jaipur 302004, India
[30]Rice University, Houston, Texas 77251
[31]Universidade de Sao Paulo, Sao Paulo, Brazil
[32]University of Science & Technology of China, Anhui 230027, China
[33]Shanghai Institute of Nuclear Research, Shanghai 201800, P.R. China
[34]SUBATECH, Nantes, France
[35]Texas A&M, College Station, Texas 77843
[36]University of Texas, Austin, Texas 78712
[37]Valparaiso University, Valparaiso, Indiana 46383
[38]Variable Energy Cyclotron Centre, Kolkata 700064, India
[39]Warsaw University of Technology, Warsaw, Poland
[40]University of Washington, Seattle, Washington 98195
[41]Wayne State University, Detroit, Michigan 48201
[42]Institute of Particle Physics, CCNU (HZNU), Wuhan, 430079 China
[43]Yale University, New Haven, Connecticut 06520
[44]University of Zagreb, Zagreb, HR-10002, Croatia

(Dated: August 29, 2003)

We present the first large-acceptance measurement of event-wise $\langle p_t \rangle$ fluctuations in Au-Au collisions at $\sqrt{s_{NN}} = 130$ GeV. Significant nonstatistical fluctuations are observed. The measured fractional $r.m.s.$ width excess of the event-wise $\langle p_t \rangle$ distribution for the 15% most-central events for charged hadrons within $|\eta| < 1$ and $0.15 \leq p_t \leq 2$ GeV/c is 13.7 ± 0.1(stat) ± 1.3(syst)% relative to a statistical reference. The variation of charge-independent fluctuation excess with centrality is non-monotonic but smooth. Charge-dependent nonstatistical fluctuations are also observed.

PACS numbers: 24.60.-k, 24.60.Ky, 25.75.-q, 25.75.Gz

Fluctuation analysis of heavy-ion collisions has been advocated to search for critical phenomena near the quantum-chromodynamic (QCD) phase boundary. Strong dependence of nonstatistical fluctuations on centrality, energy, or projectile size could form a direct indication of a transition to a quark-gluon plasma (QGP) [1, 2, 3, 4, 5, 6]. Nonstatistical fluctuations could also be produced in systems which are incompletely equilibrated following initial-state multiple scattering [7] or minijet production [8]. The discovery and study of these mechanisms and possibly others require a multifaceted analysis, of which this work is an initial component.

Ultrarelativistic nuclear collisions can be separated into transverse and axial (collision axis) phase spaces. Transverse phase space (including transverse momentum magnitude p_t and azimuth angle ϕ) for a small

pseudorapidity (η) interval is here treated as a quasi-independent thermodynamic system, for which the event-wise global variable $\langle p_t \rangle$ is a temperature estimator. For a single event with multiplicity N, it is defined as $\langle p_t \rangle \equiv 1/N \sum_{i=1}^{N} p_{t,i}$, where i is a particle index. Its distribution over an event ensemble depends on collision dynamics and the extent of equilibration. In this Letter we report the first large-acceptance measurement of $\langle p_t \rangle$ fluctuations in unidentified charged hadrons for central and minimum-bias ensembles of Au-Au collisions at $\sqrt{s_{NN}} = 130$ GeV per nucleon-nucleon pair obtained with the STAR detector at the Relativistic Heavy Ion Collider (RHIC). The STAR results are also compared with the PHENIX experiment at RHIC and experiments at the CERN Super Proton Synchrotron (SPS).

Data for this analysis were obtained with the STAR detector using a 0.25 T uniform magnetic field parallel to the beam axis. Event triggering with the central trigger barrel (CTB) scintillators and zero-degree calorimeters is described in [9], along with discussions of charged-particle kinematic measurements with the time projection chamber (TPC). Tracking efficiency was determined to be 80 - 95% within $|\eta| < 1$ and $p_t > 200$ MeV/c by embedding simulated tracks in real-data events [10], and was uniform in azimuth to 3% (*r.m.s.*) over 2π. Split-track removal required the fraction of valid space points in a track fit to be $> 50\%$. A primary event vertex within 75 cm of the axial center of the TPC was required. Valid TPC tracks fell within the full detector acceptance, defined here by $0.15 < p_t < 2.0$ GeV/c, $|\eta| < 1$ and 2π in azimuth. Primary tracks were defined as having a distance of closest approach less than 3 cm from the reconstructed primary vertex, including a large fraction of true primary hadrons and some background contamination.

This analysis consists of graphical and numerical comparisons of data to a precision statistical reference based on the central limit theorem (CLT). The CLT relates cumulants of a mean-value distribution of *independent n-samples from a fixed parent distribution* (CLT conditions) to cumulants of the parent distribution [11]. Such a mean-value distribution, equivalent to an n-folding of the parent distribution, constitutes the CLT reference. The parent distribution for this analysis is estimated by the inclusive p_t distribution (all accepted particles from all events in a centrality bin) and for the present purpose is well approximated by a gamma distribution with folding index $\alpha_0 \approx 2$. Differences between this gamma and the parent data distribution in the higher cumulants due to p_t acceptance cuts and physics correlations are strongly suppressed in the mean-value distribution comparison by inverse powers of event multiplicity and are not significant for central Au+Au collisions. Because the n-folding of a gamma distribution is itself a gamma distribution, the $\langle p_t \rangle$ reference distribution is [12]

$$g_{\bar{n}}(\langle p_t \rangle) = \frac{\alpha_0}{\hat{p}_t} \cdot \frac{e^{-\alpha_0 \bar{n} \langle p_t \rangle / \hat{p}_t}}{\Gamma(\alpha_0 \bar{n})} \cdot \left(\alpha_0 \bar{n} \frac{\langle p_t \rangle}{\hat{p}_t} \right)^{\alpha_0 \bar{n} - 1}, \quad (1)$$

where $\hat{p}_t$ and $\sigma^2_{\hat{p}_t}$ are respectively the mean and variance of the inclusive p_t distribution, $\alpha_0 \equiv \hat{p}_t^2 / \sigma^2_{\hat{p}_t}$ and $\bar{n}$ is the mean event multiplicity.

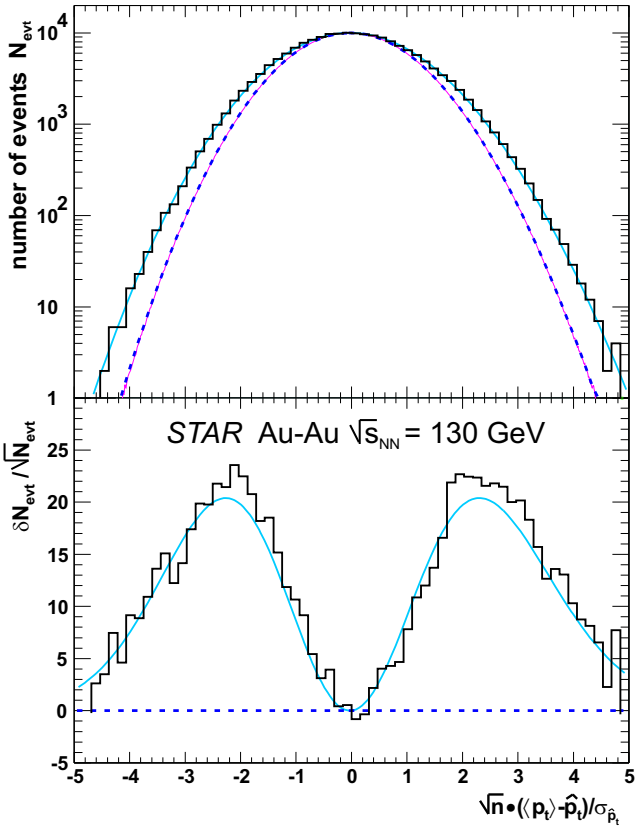

FIG. 1: Upper panel: Event-number distribution on $\sqrt{n}(\langle p_t \rangle - \hat{p}_t)/\sigma_{\hat{p}_t}$ for 80% of primary charged hadrons in $|\eta| < 1$ for 183k central events (histogram) compared to CLT gamma reference (dashed curve), Monte Carlo CLT reference (solid curve underlying gamma reference), and broadened gamma distribution (solid curve underlying data) [13]. Lower panel: Difference in upper panel between data and gamma reference (histogram) or between broadened gamma and gamma reference (solid curve) divided by Poisson error.

Fig. 1 (upper panel) shows a histogram of the number of events on $\sqrt{n}(\langle p_t \rangle - \hat{p}_t)/\sigma_{\hat{p}_t}$ for all accepted primary charged particles in 183k central Au+Au events at $\sqrt{s_{NN}}$ = 130 GeV (15% most-central events triggered by scintillator hits in the STAR CTB [9]), a CLT-reference gamma distribution (dashed curve - Eq. (1)), a Monte Carlo reference of means computed from n-fold sampling of an interpolated histogram of the experimental inclusive p_t distribution (solid curve underlying dashed curve), and a broadened gamma distribution (solid curve underlying data histogram) with width determined by the numerical analysis described below [13]. Curves are normalized to match data near the peak value, emphasizing the width comparison – the main issue of this paper. Variable $\sqrt{n}(\langle p_t \rangle - \hat{p}_t)/\sigma_{\hat{p}_t}$ in Fig. 1 minimizes bias due to multiplicity fluctuations by exploiting CLT conditions in its definition [11]. Parameters of Eq. (1) for the dashed curve are $\bar{n} = 735$, $\hat{p}_t = 535.32 \pm 0.05$ MeV/c,

and $\sigma_{\hat{p}_t} = 359.54 \pm 0.03$ MeV/c (both uncorrected for p_t acceptance cuts and inefficiencies). Data represent $80 \pm 5\%$ of the actual primary particles within the acceptance. Fig. 1 lower panel shows the difference between data and gamma reference normalized to Poisson standard deviations, emphasizing the large bin-wise significance of the variance excess. We observe very significant nonstatistical charge-independent fluctuations relative to the CLT gamma reference, but no significant deviations (bumps) from the broadened gamma distribution in Fig. 1 which might indicate the presence of anomalous event classes [1].

We apply the same central-limit approach to a numerical analysis of $\langle p_t \rangle$ fluctuations, employing as reference an algebraic analog to the gamma distribution. The statistic Φ_{p_t} [14, 15] was proposed to measure nonstatistical $\langle p_t \rangle$ fluctuations in heavy-ion collisions. In [16] Φ_{p_t} was identified as an invocation of the central limit theorem. The related *difference factor* $\Delta\sigma_{p_t\,n}$ is used in the present data analysis for reasons explained below. A numerical measure of the variance increase in Fig. 1 is defined by

$$\Delta\sigma^2_{p_t n} \equiv 2\sigma_{\hat{p}_t}\Delta\sigma_{p_t n} \equiv \frac{1}{\varepsilon}\sum_{j=1}^{\varepsilon} n_j \left[\langle p_t\rangle_j - \hat{p}_t\right]^2 - \sigma^2_{\hat{p}_t}, \quad (2)$$

where ε is the number of events in a centrality bin, j is the event index, and n_j and $\langle p_t\rangle_j$ are respectively the number and mean-p_t of accepted particles in event j. Eq. (2) is based on the CLT as a statement of scale (bin size) invariance [16], and is motivated as follows.

If detector acceptance Δx is divided into bins of size (scale) δx (*e.g.,* $\Delta\eta, \Delta\phi$ acceptance ranges and $\delta\eta, \delta\phi$ bin sizes), fluctuations of $p_{t,\alpha}(\delta x) \equiv \sum_i p_{t,\alpha i}$ (scalar p_t sum over all particles in bin α) *relative to* $n_\alpha(\delta x)$ (multiplicity in bin α) could be measured by ratio $\langle p_t\rangle_\alpha = p_{t,\alpha}(\delta x)/n_\alpha(\delta x)$. However, to minimize systematic error (bias) caused by fluctuations in $n_\alpha(\delta x)$ we introduce, as in Fig. 1, *difference variable* $p_{t,\alpha}(\delta x) - n_\alpha(\delta x)\,\hat{p}_t$ which is much less prone to this bias than ratio $\langle p_t\rangle_\alpha$. The *total variance* of this difference variable is defined by

$$\Sigma^2_{p_t\,n}(\Delta x, \delta x) \equiv \overline{\sum_{\alpha=1}^{M(\Delta x,\delta x)} (p_{t,\alpha}(\delta x) - n_\alpha(\delta x)\,\hat{p}_t)^2}, \quad (3)$$

where α is a bin index, $M(\Delta x, \delta x)$ is the event-wise number of *occupied* bins in the acceptance, and the bar denotes average over all events. Total variance is invariant on δx (at fixed acceptance) when CLT conditions are met, equivalent to the n-folding property of the gamma distribution, and is approximately factorized by

$$\Sigma^2_{p_t n}(\Delta x, \delta x) \simeq \bar{N}(\Delta x)\overline{(p_t(\delta x) - n(\delta x)\,\hat{p}_t)^2/n(\delta x)}. \quad (4)$$

The bar in Eq. (4) denotes an average over all occupied bins in all events, $\bar{N}(\Delta x)$ is the mean total event multiplicity in the acceptance, and the second factor in Eq. (4) is equivalent to the first term in Eq. (2), when evaluated at the acceptance scale. Factorization of acceptance and scale dependencies in Eq. (4) is desirable [17]. At small enough scale all non-vanishing bin occupancies go to unity and $\Sigma^2_{p_t\,n}(\Delta x, \delta x \approx 0) \to \bar{N}(\Delta x)\,\sigma^2_{\hat{p}_t}$, which also defines the inclusive variance $\sigma^2_{\hat{p}_t}$. The total-variance difference between two scales integrates correlations (due to nonstatistical fluctuations, quantum statistics, dynamics, *etc.*) within the scale interval: $\Delta\Sigma^2_{p_t\,n}(\Delta x, \delta x_1, \delta x_2) \equiv \Sigma^2_{p_t\,n}(\Delta x, \delta x_2) - \Sigma^2_{p_t\,n}(\Delta x, \delta x_1)$. $\Delta\Sigma^2_{p_t\,n} \equiv 0$ for CLT conditions in $[\delta x_1, \delta x_2]$ which establishes the numerical reference for fluctuation measurement. Taking the limiting case $\delta x_1 \approx 0$ and $\delta x_2 \to \delta x$, the total variance difference is given by $\Delta\Sigma^2_{p_t\,n}(\Delta x, \delta x) \simeq \bar{N}(\Delta x) \cdot \Delta\sigma^2_{p_t\,n}(\delta x)$, with *variance difference* $\Delta\sigma^2_{p_t\,n}(\delta x)$ and difference factor $\Delta\sigma_{p_t\,n}(\delta x)$ defined by Eq. (2) for $\delta x \to \Delta x$.

It follows from $\Delta\sigma^2_{p_t\,n} \simeq (\Phi_{p_t} + \sigma_{\hat{p}_t})^2 - \sigma^2_{\hat{p}_t}$[16] that $\Phi_{p_t}(\delta x) \simeq \Delta\sigma_{p_t\,n}(\delta x)$. Fluctuation measure $\sigma^2_{p_t,dyn}(\Delta x, \delta x) \equiv \overline{\langle (p_{t,i} - \hat{p}_t)(p_{t,j} - \hat{p}_t)\rangle_{i\neq j}}$ [18] is related to $\Delta\sigma^2_{p_t\,n}$ by $\sigma^2_{p_t,dyn}(\Delta x, \delta x) \simeq \Delta\sigma^2_{p_t\,n}(\delta x)/(\bar{N}(\Delta x) - 1)$ for approximately constant event-wise multiplicities. Φ_{p_t} and $\sigma^2_{p_t,dyn}$ may include significant dependence on multiplicity fluctuations in the case of small bin multiplicities (*e.g.*, for any bins within peripheral A-A events or for small-scale bins within central events). Variance difference $\Delta\sigma^2_{p_t\,n}(\delta x)$ is minimally biased compared to the preceding quantities.

If $p_{t,\alpha}(\delta x)$ and $n_\alpha(\delta x)$ are separable by charge species then total variances for like- and unlike-sign factors in Eq. (4) are related by $\Sigma^{2(\pm)} = \Sigma^2_{++} + \Sigma^2_{--} \pm 2\Sigma^2_{+-}$, yielding the basic relationships for this analysis:

$$\bar{N}\,\Delta\sigma^{2(\pm)} \equiv \bar{N}_+\,\Delta\sigma^2_{++} + \bar{N}_-\,\Delta\sigma^2_{--} \pm 2\sqrt{\bar{N}_+\bar{N}_-}\,\Delta\sigma^2_{+-}, \quad (5)$$

with $\Delta\sigma^{2(\pm)} \equiv 2\sigma_{\hat{p}_t}\Delta\sigma^{(\pm)}$ and $\Delta\sigma^2_{ab} \equiv 2\sqrt{\sigma_{\hat{p}_t,a}\,\sigma_{\hat{p}_t,b}}\Delta\sigma_{ab} \equiv \overline{[(p_{ta} - n_a\,\hat{p}_{ta})(p_{tb} - n_b\,\hat{p}_{tb})/\sqrt{n_a\,n_b}} - \sigma^2_{\hat{p}_t,a}\delta_{ab}]$, where $a, b = \pm, \pm$ and δ_{ab} is a Kronecker delta. Variance difference $\Delta\sigma^{2(+)}$ (like+unlike charges, also defined in Eq. (2)) measures charge-independent fluctuations, while $\Delta\sigma^{2(-)}$ (like $-$ unlike charges) measures charge-dependent fluctuations.

In this first large-acceptance analysis of $\langle p_t\rangle$ fluctuations we apply Eqs. (2) and (5) at the acceptance scale ($\delta x \to \Delta x$) to 15% most-central events (based on CTB hits) and to a minimum-bias ensemble. The object of study is the correlation state of *all* primary charged hadrons emitted into the detector acceptance. We estimate the effects of background and inefficiencies and extrapolate to the 'true' number of primaries. Difference factors for observed primary charged particles for the 15% most-central events and full acceptance are $\Delta\sigma^{(+)}_{p_t n} = 52.6 \pm 0.3$(stat) MeV/$c$ and $\Delta\sigma^{(-)}_{p_t n} = -6.6 \pm 0.6$(stat) MeV/$c$. Charge independent values of Φ_{p_t} and $\sigma^2_{p_t,dyn}$ are respectively 52.6 ± 0.3(stat) MeV/c and 52.3 ± 0.3(stat) (MeV/c)^2 (note units) for the same data; multiplicity fluctuation bias effects are small in this case. $\Delta\sigma^{(+)}_{p_t n}$ for $\bar{N} = 735$ was used to determine the solid curves in Fig. 1 underlying the data histograms, which

demonstrates consistency between the graphical results in Fig. 1 and the numerical analysis. The corresponding *r.m.s.* width increase relative to the CLT reference is $13.7 \pm 0.1(\text{stat}) \pm 1.3(\text{syst})\%$. $\Delta\sigma^{(\pm)}_{p_t n}$ were estimated to be a factor 1.26 larger in magnitude for extrapolation to 100% of primary particles for most-central events, resulting in a corrected charge-independent *r.m.s.* width increase of $17 \pm 2(\text{syst})\%$.

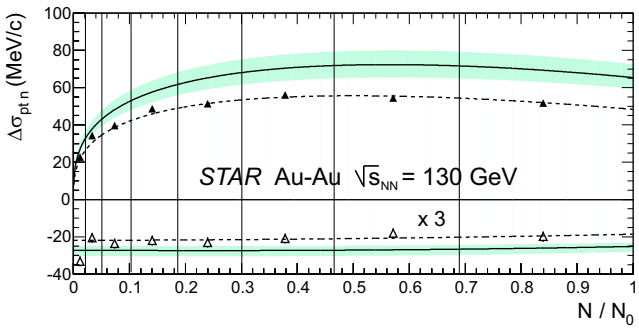

FIG. 2: Mean-p_t difference factors $\Delta\sigma^{(\pm)}_{p_t n}$ for 205k minimum-bias Au+Au events at $\sqrt{s_{NN}} = 130$ GeV versus relative multiplicity N/N_0 [10, 19]. Charge-independent (solid points) and charge-dependent (open points - multiplied by 3 for clarity) difference factors include statistical errors only (smaller than symbols). Parameterizations (dashed curves), extrapolation to true primary particle number (solid curves) and systematic uncertainties (bands) are discussed in the text.

Eight centrality classes (equal fractions of $87 \pm 2\%$ of σ_{tot}) for 205k minimum-bias events were defined by track multiplicity in $|\eta| \leq 0.5$ [10, 19]. $\Delta\sigma^{(\pm)}_{p_t n}$ values are shown as points in Fig. 2 plotted at mean multiplicities $\bar{N}$ in $|\eta| \leq 1$ for each centrality class relative to N_0, the multiplicity distribution endpoint [19]. Data points include statistical errors only (typically ± 0.5 MeV/c) and were fit with parameterizations (dashed curves) extrapolated by amounts varying from 1.17 to 1.26 (for peripheral to central events respectively) to 100% of primary charged hadrons (solid curves). The charge-independent difference factor has a very significant non-monotonic dependence on centrality, but with no sharp structure. The charge-dependent difference factor is significantly negative and approximately constant in magnitude with centrality. Charge symmetry, $\Delta\sigma_{p_t n++} = \Delta\sigma_{p_t n--}$ within statistical errors, is observed. Φ_{p_t} and $\sigma^2_{p_t,dyn}(\bar{N}-1)/2\sigma_{\hat{p}_t}$ agree with $\Delta\sigma^{(\pm)}_{p_t n}$ within statistical errors for the upper six centrality classes, but both differ from $\Delta\sigma^{(\pm)}_{p_t n}$ and each other by amounts much greater than statistical uncertainty for the two most peripheral bins, as expected from multiplicity fluctuation bias.

Systematic errors from two-track inefficiency, primary-vertex transverse position uncertainty, TPC drift speed/time-offset uncertainty and conversion electrons were estimated by Monte Carlo [20] as less than 4% of reported values. Stability of results against primary-vertex axial position variation, momentum resolution, and TPC central membrane track crossing was determined to be 5% of stated values. Effects of detector time dependence were studied by analyzing sequential run blocks (consistent within statistical error). An upper limit of 1% of reported values from collision azimuthal asymmetries within the full STAR acceptance was established by reducing the effective azimuth acceptance with track cuts to maximize sensitivity to a possible quadrupole component, mentioned further in the PHENIX comparison discussed below. Nonprimary background (∼7%) [10] added ±7% systematic error due to uncertainty in correlation content. Total systematic uncertainty for the $\Delta\sigma^{(\pm)}_{p_t n}$ data in Fig. 2 is ±9%. Detection inefficiency due to imperfect tracking and cuts was compensated in the estimate of $\Delta\sigma^{(\pm)}_{p_t n}$ for 100% of primary particles by extrapolating a trend determined by discarding tracks randomly. Extrapolation uncertainty (±8%) is dominated by uncertainty in the actual primary particle yield [10]. Total uncertainty in extrapolated values is about ±12% (shaded bands in Fig. 2). Systematic error in the most peripheral bin is larger by an additional $\sim \pm 1$ MeV/c due to possible primary-vertex reconstruction bias. Data in Fig. 2 were not corrected for two-track inefficiencies, which would increase all results in a positive sense by up to 3 MeV/c. Variations ($\approx 10\%$) in $\hat{p}_t$ and $\sigma^2_{\hat{p}_t}$ with collision centrality were accommodated by independent analyses in small centrality bins. Monte Carlo [20] estimates indicate that combined corrections for quantum and Coulomb correlations, resonances (ρ^0, ω), and $\hat{p}_t$ centrality dependence would *increase* the absolute magnitudes of all data in Fig. (2) by as much as ≈ 6 MeV/c.

SPS ($\sqrt{s_{NN}} \approx 17$ GeV) charge-independent Φ_{p_t} measurements for central A+A collisions include 0.6 ± 1.0 MeV/c for $\bar{N} \simeq 270$ in $y_{\pi,cm} \in [1.1, 2.6]$ [15] and $3.3 \pm 0.7^{+1.8}_{-1.6}$ MeV/c for $\bar{N} \simeq 162$ in $\eta_{lab} \in [2.2, 2.7]$ [21]. STAR measures $\Delta\sigma^{(+)}_{p_t n} \sim 14 \pm 2$ MeV/c for $\bar{N} \sim 180$ at the CERES [21] η acceptance. All three measurements were corrected for small-scale correlations and two-track inefficiencies. STAR results for $\Delta\sigma^{(+)}_{p_t n}$ at RHIC represent a striking increase over SPS results. In contrast, STAR $\Delta\sigma^{(-)}_{p_t n}$ is not significantly greater than the NA49 result -8.5 ± 1.5 MeV/c in $y_{\pi,cm} \in [1.1, 2.6]$ [22]. PHENIX reports charge-independent $\Phi_{p_t} \approx 6 \pm 6$ (syst) MeV/c for top 5% central events with acceptance $|\eta| < 0.35$, $\Delta\phi = 58.5°$ [23]. STAR measures $\Delta\sigma^{(+)}_{p_t n} \sim 9 \pm 1$ MeV/c at the PHENIX η, ϕ acceptance, which is greater than would be expected from a naive scaling argument because of substantial nonlinear azimuth-scale-dependent $\langle p_t \rangle$ fluctuations. HIJING [8] predicts a range of $\Delta\sigma^{(+)}_{p_t n}$ values up to one-half the reported measurements, depending on jet production and quenching options, all of which are constant with collision centrality [24].

This first large-acceptance measurement of $\langle p_t \rangle$ fluctuations at RHIC reveals intriguing deviations from a central-limit statistical reference. We observe a striking $17 \pm 2\%$ (stat+syst) *r.m.s.* excess of charge-independent fluctuations in $\sqrt{n}(\langle p_t \rangle - \hat{p}_t)/\sigma_{\hat{p}_t}$ (extrapolated to 100%

of primary charged particles in the acceptance for the 15% most-central events). The fluctuation excess varies smoothly and nonmonotonically with centrality. Charge-dependent fluctuations are smaller in magnitude and show little centrality dependence. We speculate that these fluctuations may be a consequence of hierarchical p_t production (initial-state scattering followed by parton cascade) in the early stage of the collision which have not fully equilibrated prior to kinetic decoupling [24]. Charge-dependent $\langle p_t \rangle$ fluctuations reveal nontrivial isospin-dependent correlations. Comparison with SPS experiments indicates that charge-independent fluctuations are qualitatively larger at RHIC, whereas charge-dependent fluctuations are not. A recent PHENIX result for charge-independent fluctuations, although compatible with zero within their systematic error, is consistent with a significant non-zero STAR measurement restricted to the PHENIX acceptance.

We thank the RHIC Operations Group and RCF at BNL, and the NERSC Center at LBNL for their support. This work was supported in part by the HENP Divisions of the Office of Science of the U.S. DOE; the U.S. NSF; the BMBF of Germany; IN2P3, RA, RPL, and EMN of France; EPSRC of the United Kingdom; FAPESP of Brazil; the Russian Ministry of Science and Technology; the Ministry of Education and the NNSFC of China; SFOM of the Czech Republic, DAE, DST, and CSIR of the Government of India; the Swiss NSF.

[1] R. Stock, Nucl. Phys. **A661**, 282c (1999); H. Heiselberg, Phys. Rep. **351**, 161 (2001).
[2] M. Asakawa, U. Heinz, B. Müller, Phys. Rev. Lett. **85**, 2072 (2000).
[3] S. Jeon, V. Koch, Phys. Rev. Lett. **85**, 2076 (2000).
[4] M. Stephanov, K. Rajagopal, E. Shuryak, Phys. Rev. D **60**, 114028 (1999).
[5] A. Dumitru, R. Pisarski, Phys. Lett. **B504**, 282 (2001).
[6] L. M. Bettencourt, K. Rajagopal and J. V. Steele, Nucl. Phys. **A693**, 825 (2001).
[7] M. Gaździcki, A. Leonidov, G. Roland, Eur. Phys. J. **C6**, 365 (1999).
[8] X.-N. Wang, M. Gyulassy, Phys. Rev. D **44**, 3501 (1991).
[9] K. H. Ackermann *et al.*, Nucl. Instrum. Meth. A **499**, 624 (2003); see other STAR papers in volume A**499**.
[10] C. Adler *et al.*, Phys. Rev. Lett. **87**, 112303 (2001); *ibid.* **89**, 202301 (2002).
[11] *E.g.,* for CLT conditions $\overline{\langle p_t \rangle} = \hat{p}_t$ and $\sigma^2_{\langle p_t \rangle} = \sigma^2_{\hat{p}_t}/\bar{n}$, where $\hat{p}_t$ and $\sigma^2_{\hat{p}_t}$ are the mean and variance, respectively, of the parent p_t distribution and $\overline{\langle p_t \rangle}$ and $\sigma^2_{\langle p_t \rangle}$ are the mean and variance of the $\langle p_t \rangle$ distribution.
[12] M.J. Tannenbaum, Phys. Lett. **B498**, 29 (2001).
[13] The upper solid curve in Fig. 1 was obtained by raising the reference gamma distribution to the power, $(1 + \Delta\sigma^2_{p_t n}/\sigma^2_{\hat{p}_t})^{-1}$, and normalizing to data at the maximum.
[14] M. Gaździcki, St. Mrówczyński, Z. Phys. C **54**, 127 (1992).
[15] H. Appelshäuser *et al.* (NA49 Collaboration), Phys. Lett. **B459**, 679 (1999).
[16] T. A. Trainor, hep-ph/0001148.
[17] The explicit scale dependent factor in Eq. (4) does not depend on acceptance *size*, but can depend on acceptance *position*. The latter dependence on η is negligible here.
[18] S. A. Voloshin, V. Koch, H.G. Ritter, Phys. Rev. C **60**, 024901 (1999).
[19] N_0 is the half-max point at the end of the minimum-bias distribution plotted as $d\sigma/dN_{ch}^{1/4}$, and is an estimator on N for the maximum number of participant nucleons, in which case $N_{part}/N_{part,max} \simeq N/N_0$ within 4%.
[20] R. Ray and R. Longacre, nucl-ex/0008009.
[21] D. Adamová *et al.,* (CERES Collaboration), nucl-ex/0305002. CERES also reports quantity $\Sigma_{p_t} \equiv \sqrt{\Delta\sigma^2_{p_t n}/\bar{N}\hat{p}_t^2}$ with magnitude approximately half that at STAR.
[22] J. G. Reid, Ph. D. thesis, Univ. of Washington, nucl-ex/0302001.
[23] K. Adcox *et al.* (PHENIX Collaboration), Phys. Rev. C **66**, 024901 (2002).
[24] Q. Liu and T. A Trainor, Phys. Lett. **B567**, 184 (2003).